Available online at www.CivileJournal.org

Civil Engineering Journal

(E-ISSN: 2476-3055; ISSN: 2676-6957)

Vol. 12, No. 04, April, 2026

Effect of Mixing Sequence on Properties and Fibre Dispersion of Glass Fibre Reinforced Cementitious Mortar

Affif M. Sapawi [1], Abraham H. Bernard [1], Ahmad N. Rizalman [1*], S. M. Iqbal S. Zainal [1], Guan Lin [2], Zhao Danwei [3], Rosalam Sarbatly [1]

[1] *Nanomaterials Research Centre, Faculty of Engineering, Universiti Malaysia Sabah, Kota Kinabalu 88400, Sabah, Malaysia.*

[2] *Department of Ocean Science and Engineering, Southern University of Science and Technology, Guangdong 518055, China.*

[3] *Faculty of Forestry, Beihua University, Jilin City 132000, China.*

Received 08 September 2025; Revised 24 March 2026; Accepted 29 March 2026; Published 01 April 2026

Abstract

Cementitious composites play a vital role in construction due to their favourable strength, durability, and workability. Nonetheless, these materials are susceptible to cracking. Although incorporating glass fibres has improved mechanical properties, achieving uniform fibre dispersion remains a significant challenge. The objective of this study was to examine the effect of mixing sequence on the engineering properties and fibre dispersion of glass fibre–reinforced cementitious mortars (GFRCMs). There were four mixing sequences including: four mixing sequences for glass fibre-reinforced cementitious mortars (GFRCMs): (i) S1(fibres were incorporated into dry mortar mixtures), (ii) S2 (fibres were incorporated into fresh mortar mixtures), (iii) S3 (fibres added alongside gradual water addition, (iv) S4 (fibres were included during incremental water additions). This study examined various properties in accordance with the American Society for Testing and Materials (ASTM) standard test methods, including compressive strength, hardened density, setting time, flowability, and flexural strength. Scanning electron microscopy and fibre-distance analysis were also employed to evaluate the fibre dispersion of the specimens. The results indicate that fibre addition reduced the flowability and shortened the setting time of the mortar, whereas improvements in hardened properties depended strongly on dispersion quality. The most uniform fibre distribution was observed in S4 ($\beta = 0.685$), resulting in maximum compressive and flexural strengths of 15.88 MPa and 10.39 MPa, respectively, at 28 days. The strong correlations observed between density and porosity ($R^2 = 0.8035$) and between density and compressive strength ($R^2 = 0.8184$) indicate that reduced void content and enhanced fibre distribution are key contributors to the observed performance gains. This work establishes relationships among mixing sequence, fibre dispersion, and key engineering properties to guide fibre-mixing processes in cementitious composites.

Keywords: Glass Fibre Reinforced Cementitious Mortar; Fibre Dispersion; Mixing Methods; Compressive Strength.

1. Introduction

Cementitious composites (mortar and concrete) are the most widely utilised construction materials globally, owing to their favourable durability, workability, and strength [1, 2]. Nonetheless, the composites are prone to cracking. This process can then notably compromise the material's tightness, reducing its strength and durability [3, 4]. Hence, reinforcing the materials with fibres is one method to mitigate this issue. Previous studies also reported that incorporating fibres into composites can improve impact resistance, ductility, flexural strength, and tensile strength while reducing stress concentrations at crack tips [5-7].

* Corresponding author: ahmadnurfaidhi@ums.edu.my

https://doi.org/10.28991/CEJ-2026-012-04-017

Glass fibres are slender, robust strands commonly used as reinforcement in composites owing to their strength and resilience [8, 9]. These fibres predominantly consist of 45-75% silica oxide and various oxides (Al, Ca, B, and Mg) [10]. Nevertheless, only alkali-resistant (AR) glass fibre contains ZrO_2, ranging from 1 to 18% [10-12]. Numerous studies have also documented that adding glass fibre to cementitious composites decreases flowability. This outcome has been attributed to the fibre's water-absorption characteristics [13-15]. Conversely, a significant increase in the strength of the composites (attributed to stress transfer across the fibres) and an enhanced delay in crack propagation (facilitated by fibre bridging) have been observed [8, 16].

The primary concern with fibres is their tendency to aggregate in the mixture, resulting in uneven fibre dispersion in the composite. Certain studies have indicated that glass fibre clumping occurs at elevated fibre content, reaching 1% [17-21]. This clumping effect can lead to the formation of larger voids and weaker regions within the composite, thereby diminishing its strength [22-25]. Likewise, optimising the mixing duration and the sequence of fibre addition in composites is an effective method to ensure uniform fibre dispersion. Liu and Fall [26] asserted that extended mixing periods could result in more dispersed fibres and enhanced workability of fresh composite mixtures. The study stated that this process could improve the mechanical characteristics of the hardened composites. In contrast, some studies argued that prolonged mixing time could lead to fibre intertwining, thereby substantially impairing concrete flow and degrading composite properties [27-31].

Two methods have been employed to prepare cementitious composites for investigations into the sequence of fibre addition. The initial approach entails incorporating fibres into dry composite mixtures [12, 32], whereas the subsequent method consists of integrating fibres into fresh mixtures [27, 33-38]. Subsequently, this latter method has been further refined by incorporating the fibre as water that is introduced gradually in two or more phases. França et al. [34] combined fibres with cementitious materials, implementing a two-step water addition process (25% initially and 75% subsequently). The study demonstrated that incorporating fibre into entirely fresh mixtures improved rheological properties while reducing the required mixing energy. On the contrary, final torque measurements revealed that the outcomes were comparable regardless of whether water was added in two steps or all at once [34]. Gyawali [36] found that gradual water addition (in two steps) enhanced engineering features. This improvement was ascribed to the uniform distribution of fibres and their thorough coating with paste, which effectively inhibited the formation of fibre clumps.

Multiple methods have been utilised to assess the impact of the fibre addition sequence. The initial approach involves observing the flowability of the fresh mixtures, and specific studies have investigated the presence of discernible fibre lumps [36, 39-41]. Conversely, a few studies have quantified the spread-flow diameters of the mixtures to assess the impact of fibre inclusion [6, 31, 34-35, 42]. At the microscopic level, the fibre dispersion in the hardened composites has been estimated using X-ray computed tomography (CT) scanning [35] and scanning electron microscopy (SEM) [12, 32, 37]. These tools can evaluate the hardened state of the composites by assessing their strength and physical characteristics. Another test widely used to evaluate a composite's bending resistance is the flexural strength [12, 36-38].

Furthermore, the compressive strength test is typically used to assess a material's capacity to withstand axial loads [12, 32, 37, 38]. The hardened density and porosity of the composites have also been investigated primarily to understand their structural integrity [37, 38]. To the author's knowledge, there has been a deficiency of studies that quantitatively and qualitatively correlated the strength and dispersion of glass fibre in cement mortar. Thus, this study examined the relationship when glass fibre-reinforced cementitious mortars (GFRCMs) were prepared under various mixing sequences. Different test methods were also utilised, including destructive testing, imaging techniques, and statistical measurements.

2. Methodology

2.1. Materials

Figure 1 depicts the components utilised in the production of GFRCMs, consisting of Ordinary Portland cement (OPC), fine aggregate (river sand), water, superplasticiser, and AR glass fibre. The selected materials ensured optimal workability and mechanical efficiency. Meanwhile, the cement utilised was categorised as Type II and Type IIA according to ASTM C150 [43], rendering it appropriate for applications requiring moderate sulphate resistance and a regulated heat of hydration. The fine aggregate used was natural river sand, selected for its ability to improve mortar texture and overall strength. A high-range water-reducing admixture compliant with ASTM C494 Type F and British Standard European Norm (BS EN) 934-2:2001 (ADVA Cast 3865) was then applied as a superplasticiser to enhance workability [44, 45]. This superplasticiser improved flowability and mechanical characteristics while maintaining durability. Moreover, the mortar incorporated approximately 1 cm-long AR glass fibres, enhancing crack resistance and structural integrity. The water utilised also conformed to the specifications established in ASTM C1602, ensuring consistency and quality in cementitious mixtures [46].

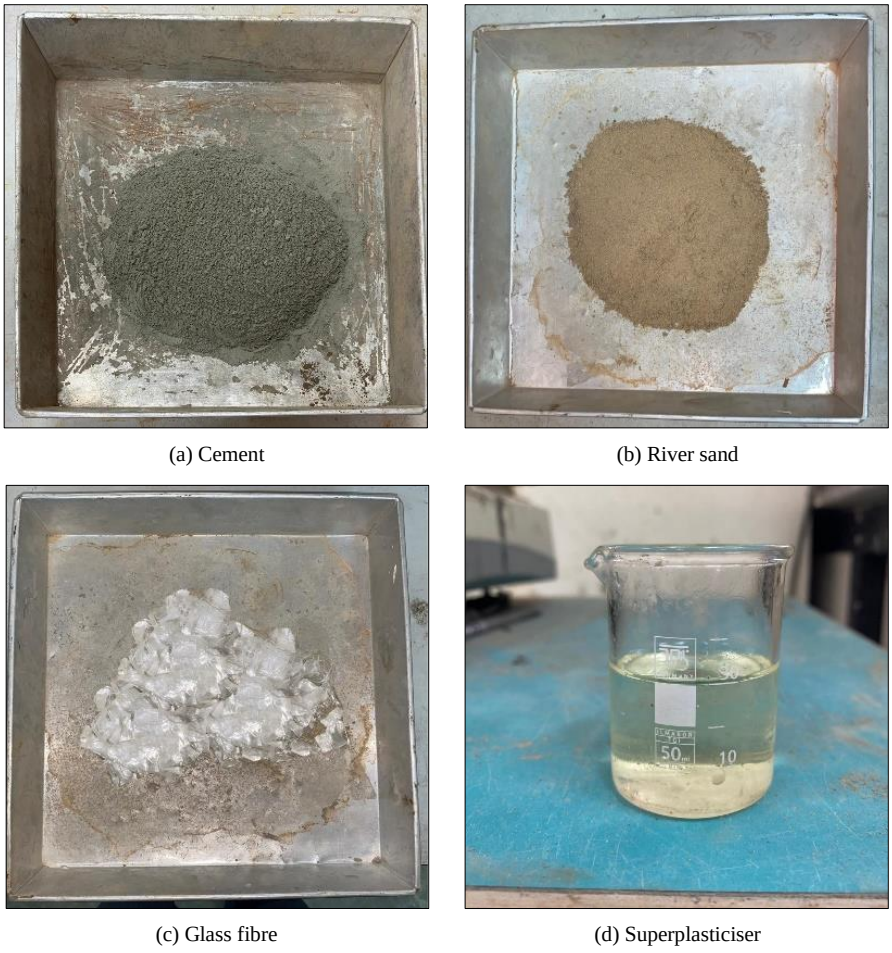

(a) Cement (b) River sand

(c) Glass fibre (d) Superplasticiser

Figure 1. The materials employed to fabricate GFRCMs, including (a) cement, (b) river sand, (c) glass fibre, and (d) superplasticiser

2.2. Mixture Proportions and Specimen Designation

Table 1 tabulates the mixture proportions for both control and GFRCMs. These specimens were prepared in accordance with ASTM C109, which involved 0.5 kg of cement, 1.375 kg of sand, and 0.243 kg of water [47]. Consequently, a water-cement (w/c) ratio of 0.485 was achieved. Glass fibre was incorporated at 1% of the cement weight (0.005 kg), a dosage fixed based on previous optimisation studies indicating that this content provides a suitable balance between mechanical enhancement and workability [14, 17–21]. In this study, the fibre volume fraction was intentionally kept constant to isolate the influence of mixing sequence on fibre dispersion and composite performance. Introducing multiple fibre dosages would introduce an additional experimental variable and obscure the specific contribution of the mixing sequence.

Table 1. Summary of the mixture proportions for the control and GFRCMs

Specimen	Percentage of Glass Fibre (%)	w/c Ratio	Mix proportions (g)				
			Fine Aggregate	Cement	Glass Fibre	Water	Superplasticiser
Cement Mortar without Fibre (Control)	0	0.485	1.375	0.5	0.000	0.356	0.00375
Cement Mortar with Fibre (GFRCMs)	1	0.485	1.375	0.5	0.005	0.356	0.00425

Considering the sand's absorption rate of 8.87%, an additional 0.122 kg of water was added to counteract moisture loss and maintain consistency in the mix. Moreover, a high-range water-reducing admixture was incorporated at 0.75% (control mix) and 0.85% (fibre-reinforced mix) to achieve the target mortar flow of 110 ± 5, as stipulated for ASTM C109 mortar preparation and verified using the flow table method (ASTM C1437) [38, 39]. For the control mixes, dosages above 0.75% caused the flow to exceed the specified range, whereas for the fibre-reinforced mixes, dosages below 0.85% were insufficient to achieve the target flow due to the additional yield stress and water demand introduced by the fibres. Therefore, the slightly higher superplasticiser dosage in the fibre mixes was selected to achieve comparable flowability, enabling evaluation of mixing sequence effects on fibre dispersion and void structure without interference from variations in initial rheology.

2.3. Mixing sequence

Figure 2 illustrates the mixing sequences utilised in this study. Several sequences are designed as follows:

- Sequence 1 (S1) involved adding glass fibres to the dry mixtures of cement and sand.
- Sequence 2 (S2) involved adding glass fibres into the fresh mixtures of cement and sand.
- Sequence 3 (S3) involved adding glass fibres into fresh mixtures, with water added incrementally.
- Sequence 4 (S4) involved adding glass fibres between successive water additions.

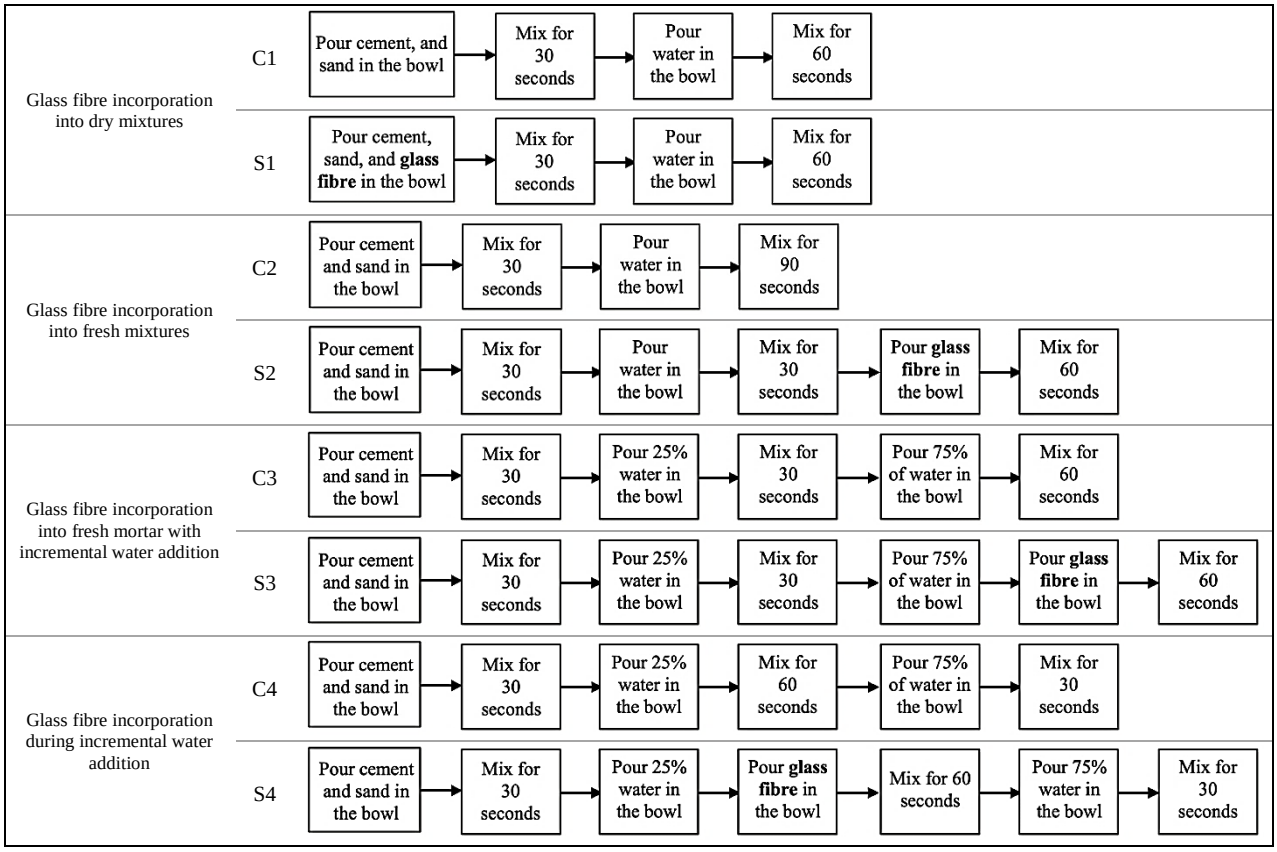

Figure 2. Summary of the mixing sequences utilised in this study

A comparative analysis was also performed by fabricating four control specimens (C1, C2, C3, and C4) to correspond to S1, S2, S3, and S4, respectively. These mixing sequences followed the method reported by França et al. [34]. To ensure reproducibility and minimise unintended changes in mixing energy, all batches were mixed using the same laboratory mortar mixer at a constant rotational speed of 185 rpm, following the optimum mixing speed reported by Choi & Yuan [18] for fibre-reinforced cementitious composites. The sequences differ only in the order of fibre and water addition and, consequently, in the number of mixing steps required to reach a homogeneous mixture. S1 used a total mixing time of 90 s, where fibres were pre-blended with the dry constituents, allowing rapid fibre separation before wetting. For S2–S4, the total mixing time was 120 s to accommodate the additional step(s) of fibre incorporation and/or staged water addition while ensuring complete wetting, paste coating, and re-homogenisation after each addition. Pilot trials indicated that using only 90 s for S2–S4 led to incomplete fibre wetting and visible fibre clusters, whereas extending beyond 120 s increased the risk of fibre entanglement and unnecessary workability loss; thus, 120 s was adopted as a practical compromise to achieve consistent mixing quality across staged sequences.

This study examined the characteristics of fresh mortar (flowability and setting time) in accordance with ASTM C1437 and ASTM C191 [48, 49]. The fresh mortar was initially cast into cube moulds measuring 50 mm × 50 mm × 50 mm and prism moulds measuring 160 mm × 40 mm × 40 mm. Each specimen was then subjected to 30 s of platform vibration following casting to remove air bubbles while ensuring adequate compaction. Subsequently, the specimens remained in their moulds for 24 h at a controlled temperature of 20 ± 2°C to facilitate initial setting before demoulding. These specimens were submerged in a curing tank filled with water to sustain hydration conditions for 7 and 28 days following demoulding. Finally, the hardened properties of the specimens were assessed involving several variables. These variables included hardened density, compressive strength, and flexural strength in accordance with BS EN 1015-10, ASTM C109, and ASTM C348, respectively [47, 50, 51]. Table 2 summarises the measured values for the fabricated specimens. Eight specimens were analysed, with each property recorded as an average of three measurements. Each specimen comprised 15 samples, including nine cube moulds and six prisms. In total, 120 samples were composed of 72 cube moulds and 48 prisms.

Table 2. Summary of the measured values for the fabricated specimens

Specimen	Hardened Density	Compressive Strength		Flexural Strength	
	28th Day	7th Day	28th Day	7th Day	28th Day
C1	3	3	3	3	3
C2	3	3	3	3	3
C3	3	3	3	3	3
C4	3	3	3	3	3
S1	3	3	3	3	3
S2	3	3	3	3	3
S3	3	3	3	3	3
S4	3	3	3	3	3
Subtotal	**24**	**24**	**24**	**24**	**24**
Total	**120**				

2.4. Research Methods

2.4.1. Material Characterization

Numerous characteristics of the constituent materials were examined before their incorporation into the mortar mixtures. Thus, various material characterisation techniques were applied to assess the physical, chemical, and microstructural features of these materials. High-magnification images for evaluating the fibre integrity and surface condition of glass fibres were initially obtained using a field-emission scanning electron microscope (FESEM). This tool could provide information regarding the morphology and surface texture of glass fibres. Subsequently, water contact angle measurements were conducted to compute the wettability of the glass fibres. The identification of the elemental oxides in each material was also facilitated through X-ray fluorescence (XRF) spectroscopy. This tool examined the chemical compositions of glass fibre, cement, and fine aggregate. Lastly, the water absorption capacity of the river sand was determined in accordance with ASTM C128 [52]. This standard test approach could determine the specific gravity and absorption of fine aggregate. Overall, the required specifications for cementitious applications and the guided modifications to the mixture design were ensured to be compliant using these characterisation tools. This process could ensure consistency and performance.

2.4.2. Engineering Properties

This study evaluated the engineering properties regarding flowability (ASTM C1437) [48], setting time (ASTM C191) [49], hardened density (BS EN 1015-10) [50], compressive strength (ASTM C109) [47], and flexural strength (ASTM C348) [51].

2.4.3. Fibre Dispersion

This study employed three complementary methodologies to evaluate fibre dispersion as follows:

- Fracture surfaces and cross-sections of prism specimens were examined using SEM. This process facilitated the visualisation of fibre distribution while examining their interaction with the surrounding matrix.
- A quantitative evaluation was conducted using fibre distance analysis (FDA) to complement these imaging methods. The methodology utilised in this step followed the techniques reported by Betterman et al. [53]. Hence, the dispersion coefficient (β) was measured by determining the fibre spacing. This coefficient is a dimensionless indicator of distribution uniformity, with a more uniformly distributed fibre network in the hardened composite corresponding to a larger β value. The β can be determined using an equation expressed as follows:

$$\beta = e^{-\psi(x)} \quad (1)$$

where $\psi(x)$ denotes the coefficient of variation. This $\psi(x)$ can also be calculated utilising an equation formulated as follows:

$$\psi(x) = \sigma/\mu \quad (2)$$

where σ represents the standard deviation of the fibre distance from three samples, and μ represents the mean value of the fibre distance from three samples.

Figure 3 presents a flowchart that summarises the experimental procedures employed in this study.

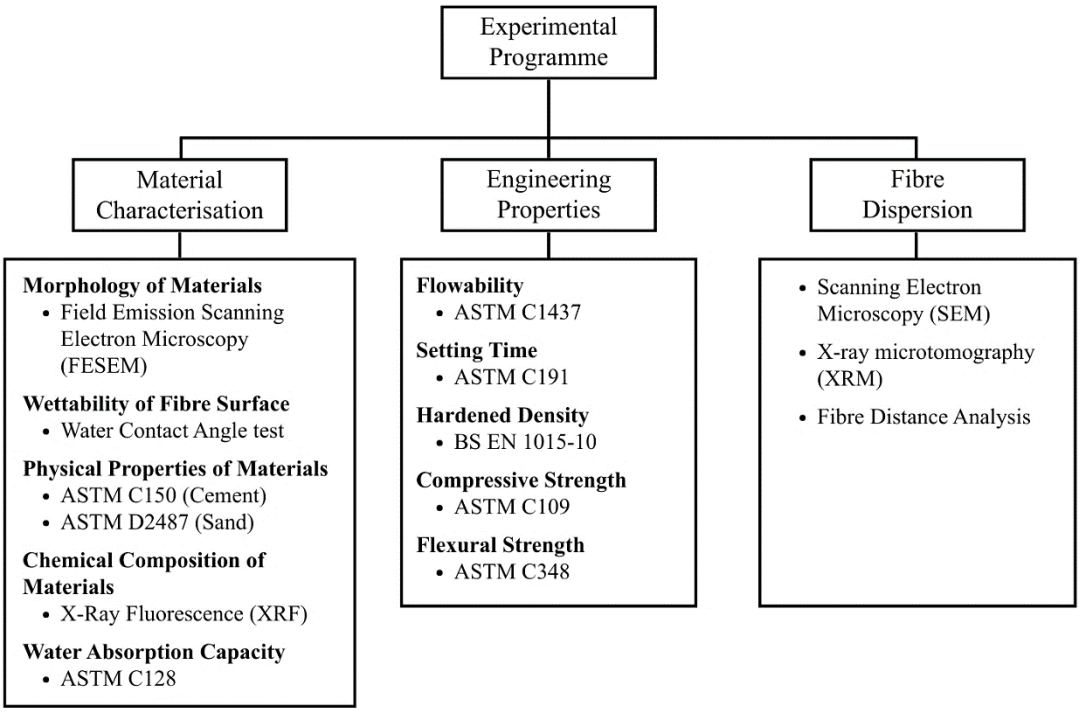

Figure 3. The experimental procedure flowchart employed in this study

3. Characterization of Materials

3.1. Microstructural Characteristics of Glass Fibre

Figure 4 displays the FESEM images of glass fibres at ×500 magnification. The diameter of the fibre ranged between 16.7 and 18.8 µm, classifying them as microfibres [54]. Given that these fibres possessed micro-scale dimensions, they effectively bridged micro-cracks. Consequently, crack widths were reduced while postponing crack initiation [55]. This property also improved the composite's fracture resistance, enhancing its durability under mechanical stress [6, 7].

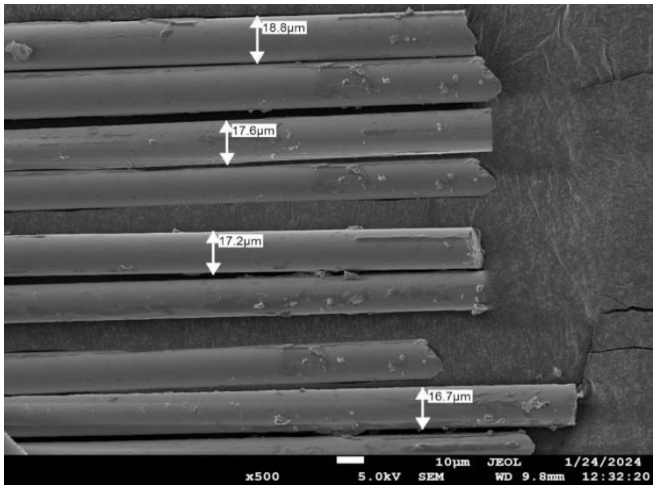

Figure 4. The diameters of glass fibres at ×500 magnification

Figure 5 illustrates that the water contact angle of the glass fibre is 61.93°, signifying a hydrophilic surface. This finding was also consistent with the outcomes reported by Li et al. [56], who similarly found that glass fibres were hydrophilic. The hydrophilic nature of the fibres could also enhance interfacial adhesion with the cement matrix, potentially increasing bonding strength. Nevertheless, increased water absorption could affect flowability and setting time, making the fibre-dispersion approach essential to achieve uniform performance. Table 3 lists the microstructural characteristics of the glass fibres.

Table 3. Summary of the microstructural characteristics of the glass fibres

Diameter (µm)	Length (mm)	Water Contact Angle (°)
16.7–18.8	10	61.93

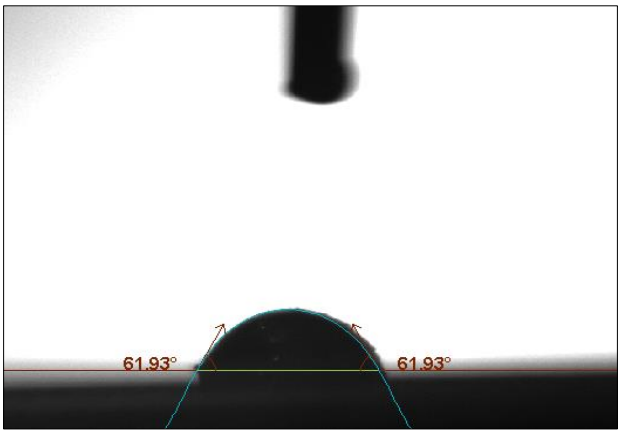

Figure 5. The water contact angle of the glass fibre

Figure 6 portrays the surface morphology of the glass fibres analysed through an SEM tool at ×500 and ×1000 magnifications. A smooth texture characterised by subtle striations was then observed. No contaminants or surface coatings were also identified, implying that the fibres maintained structural integrity during the manufacturing process. This lack of defects suggested that the fibres retained their inherent mechanical properties, ensuring uniform performance within the cementitious matrix.

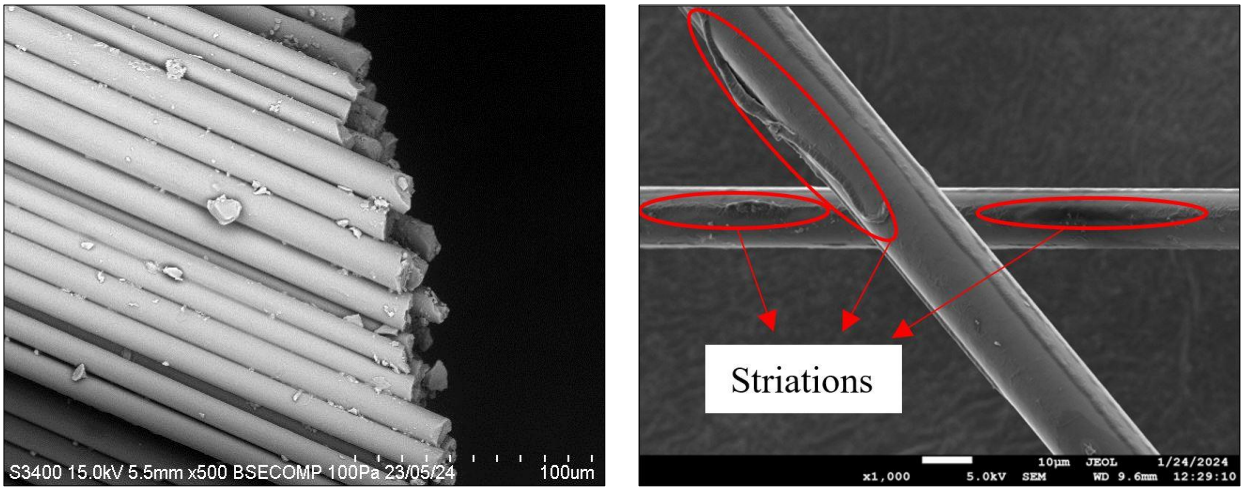

(a) (b)

Figure 6. The surface of glass fibres at (a) ×500 and (b) ×1000 magnifications

3.2. Physical Characteristics of Cement and Sand

Figures 7 and 8 present the particle size distributions of the cement and river sand, respectively, obtained from sieve analysis. As shown in Figure 7, approximately 87% of the cement particles passed the 0.045 mm (45 µm) sieve, indicating that the cement satisfied the fineness requirement and is consistent with the specification limits outlined in ASTM C150 [43]. The fine aggregate used in this study was natural river sand. Based on the distribution shown in Figure 8, 100% of the sand particles passed through the 4.75 mm sieve, confirming compliance with the ASTM D2487 [57] size classification criteria. Additionally, the river sand exhibited a water absorption rate of 8.87%, which was incorporated into the mixture design to account for moisture demand and maintain the specified w/c ratio. Table 4 summarises the physical properties of the cement and sand.

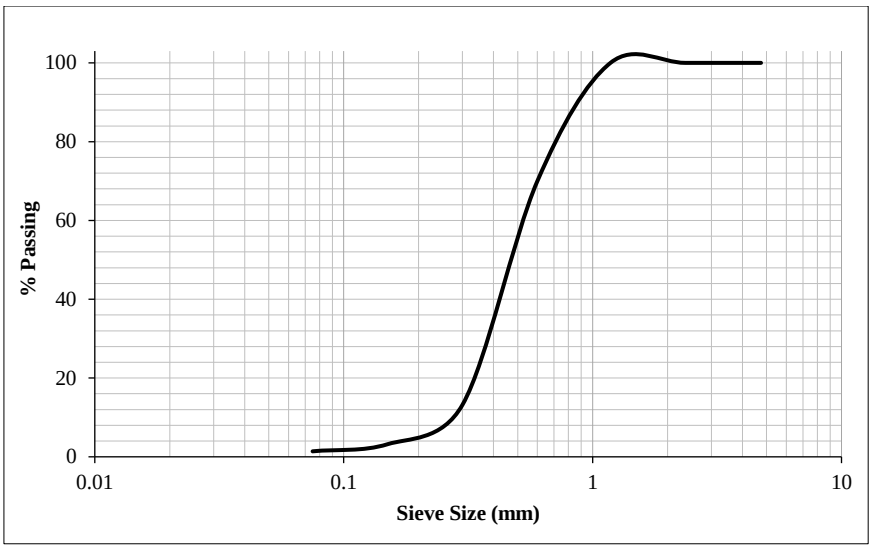

Figure 7. Particle Distribution of River Sand

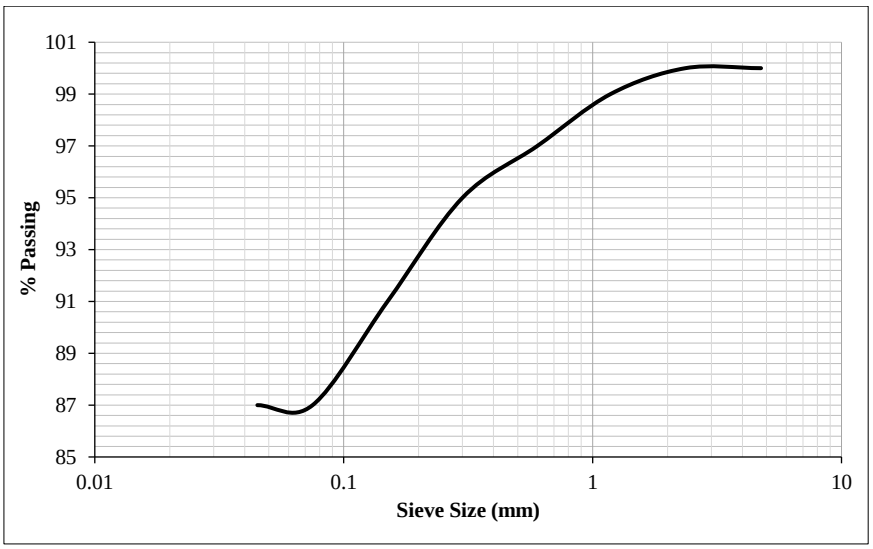

Figure 8. Particle Distribution of Cement

Table 4. Summary of the physical characteristics of cement and sand

Material	% Pass Sieve 4.75 mm	% Pass Sieve 0.045 mm	Water Absorption Rate (%)	ASTM Standard Compliance
OPC	100	87	-	ASTM C150 passed a 45 µm sieve
River Sand	100	-	8.87	ASTM D2487 passed a 4.75 mm sieve

3.3. Chemical Composition of Materials

The chemical composition of the materials used in this study influenced the mechanical performance and durability of the composite. Table 5 indicates that the glass fibre consists predominantly of SiO_2 (56.56%), confirming that silica is its primary component. This observation is a characteristic typical of most glass-based materials. The CaO content (26.06%) also implied significant thermal and mechanical stability, rendering the fibres suitable for high-temperature applications and cementitious reinforcement [58]. Alternatively, the inclusion of ZrO_2 (2.48%) improved the fibre's resistance to chemical corrosion, enhancing its fracture toughness and overall durability. The TiO_2 component also increased wear resistance and mechanical strength (even at low levels), improving the durability and performance of fibres in cementitious composites [59].

Table 5. Chemical composition summary of glass fibres

Element	SiO_2	CaO	ZrO_2	Al_2O_3	TiO_2	K_2O	P_2O_5
Percentage (%)	56.56	26.06	2.48	9.16	0.91	0.14	0.06

Table 6 presents the chemical composition of cement. The composition was primarily characterised by CaO (63.70%), which was essential for the hydration, setting, and hardening processes of the cement matrix. Likewise, the SiO_2 content (21.00%) facilitated the formation of calcium silicate hydrates (C-S-H), which were integral to strength development and long-term durability [60]. The presence of SO_3 (4.91%) also suggested the regulated incorporation of gypsum, regulating the setting time. This process could prevent premature hardening while enhancing workability [61]. Table 7 demonstrates the chemical composition of sand. The high SiO_2 content (85.25%) signified that the sand was predominantly composed of quartz. This material is a typical component of construction sand. The Fe_2O_3 (4.05%) contents also indicated impurities primarily associated with natural sand. Although these impurities could affect the colour and mechanical properties of the sand, their presence at low levels was generally deemed acceptable [62].

Table 6. Chemical composition summary of cement

Element	CaO	SiO_2	SO_3	Al_2O_3	Fe_2O_3	MgO	K_2O
Percentage (%)	63.70	21.00	4.91	3.94	3.74	1.12	0.67
Allowable Limit (ASTM C150) [43]	-	-	-	≤ 6.0	≤ 6.0	≤ 6.0	-

Table 7. Chemical composition summary of sand

Element	SiO_2	Fe_2O_3	K_2O	TiO_2	SO_3	CaO	P_2O_5
Percentage (%)	85.25	4.04	1.47	0.25	0.22	0.20	0.10

4. Engineering Properties of GFRMs

4.1. Flowability

Flowability is a crucial factor affecting the workability of fresh mortar [39]. The incorporation of glass fibres typically diminishes flowability, attributed to increased internal friction and the water-absorptive characteristics of the fibres [63]. In addition, the rough surface features observed on the glass fibres (Figure 6-b) can increase fibre-particle friction and disrupt the lubricating water film, thereby contributing to the reduction in spread flow. Figure 9 illustrates that the control specimens display greater spread-flow diameters of 22.20 cm (C1), 22.40 cm (C2), 22.30 cm (C3), and 22.50 cm (C4). Conversely, the GFRCMs exhibited diminished flowability, with spread-flow diameters measuring 21.90 cm (S1), 21.50 cm (S2), 22.00 cm (S3), and 22.10 cm (S4). In particular, the reduced flowability observed in S1 and S2 was due to increased fibre-induced viscosity, which hindered particle movement while increasing shear resistance within the cementitious matrix [63]. The increased flowability observed in S4 is consistent with the findings reported by Gyawali [36], who employed a two-stage water-addition approach in which fibres were introduced between water additions. This improvement may be attributed to the second water addition acting as free water within the fibre-reinforced mortar, thereby enhancing workability while exerting minimal influence on the coating condition of the dispersed fibres in the matrix [36].

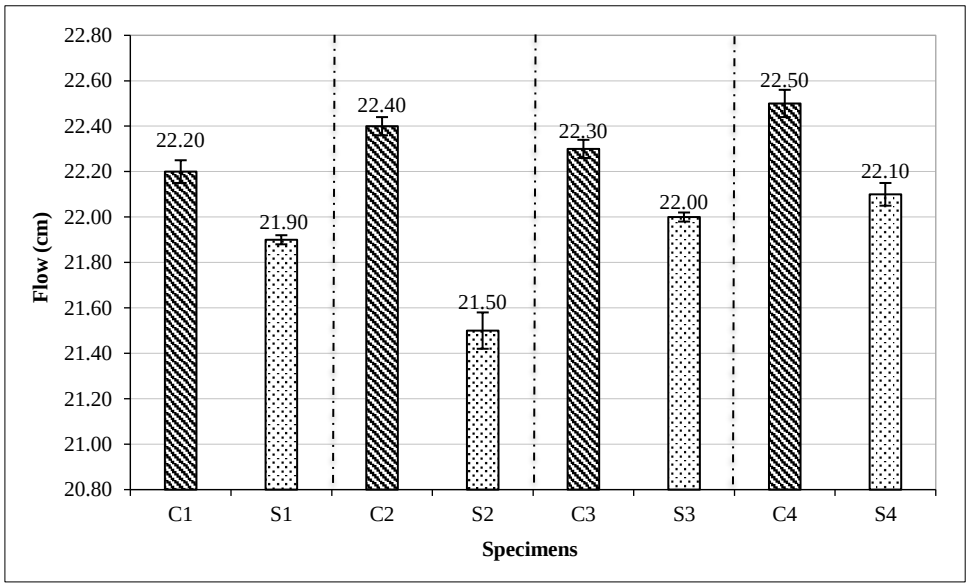

Figure 9. Graph of flowability versus specimens

4.2. Setting Time

The setting time usually denotes the period required for cementitious materials to evolve from a fresh to a hardened state, which can be influenced by hydration reactions and water availability [64]. This study indicated that the control specimens had longer setting times than the fibre-reinforced specimens. Hence, the decrease in setting time for GFRCMs was mainly due to the water-absorption capacity of glass fibres, which reduced the free water available for cement hydration [65].

Beyond this water-reduction effect, the surface characteristics of the fibres also play an important role. The fibres are hydrophilic, with a water contact angle of 61.93°, and possess a rough surface as shown in Figure 6-b. These features can locally limit water mobility and provide additional nucleation sites for early hydration products such as C–S–H at the fibre–paste interface. Such interfacial nucleation and confinement effects may further accelerate stiffening beyond that achieved by bulk water reduction alone, particularly when fibre dispersion is non-uniform and local fibre concentration is high.

Figure 10 illustrates the setting times of all specimens. The initial and final setting times of the control specimens were calculated as 195 and 240 minutes for C1, 190 and 210 minutes for C2, 240 and 255 minutes for C3, and 240 and 255 minutes for C4. In contrast, the GFRCMs consistently exhibited shorter setting times. The initial and final setting times were 175 and 190 minutes for S1, 145 and 160 minutes for S2, 215 and 230 minutes for S3, and 230 and 245 minutes for S4.

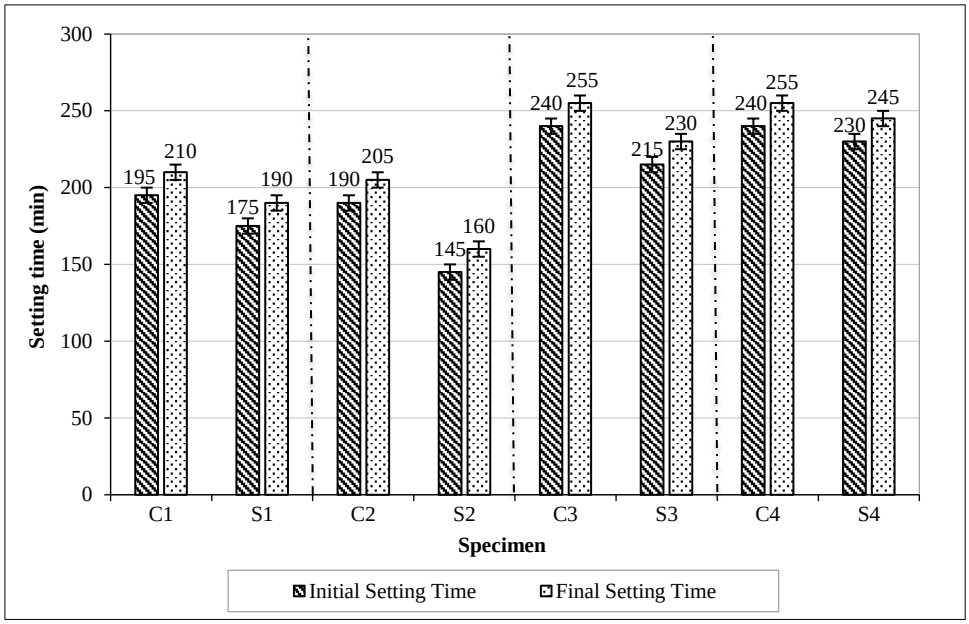

Figure 10. Graph of setting time versus specimens

Zainal et al. [12] proposed that water absorption effects could stem from uneven material distribution. Concurrently, the study noticed that reduced setting times in GFRCMs could be another observable outcome. This process could then enhance heat dissipation and cooling. Notably, S4 demonstrated the longest setting time in this study. This finding was likely due to the improved cement particle coating and fibre dispersion within the mixing approach. The reduction in rapid heat dissipation noted in S1 and S2 could also be attributed to the incremental addition of water, which facilitated more consistent hydration. Furthermore, reduced excessive water absorption, decreased overall hydration rate, and prolonged setting time were observed in S4 owing to the improved fibre distribution.

4.3. Hardened Density and Porosity

The strength and durability of cementitious composites depend on their hardened density. Increased density usually indicates reduced voids and enhanced compaction, thereby improving mechanical characteristics and durability [42]. Figure 11 shows that all GFRCMs exhibit greater density than the control specimens, with S4 exhibiting the highest density. S3, S1, and S2 succeeded this outcome. Therefore, the S4 mixing sequence likely enhanced fibre dispersion, resulting in a denser, more compact material with fewer voids.

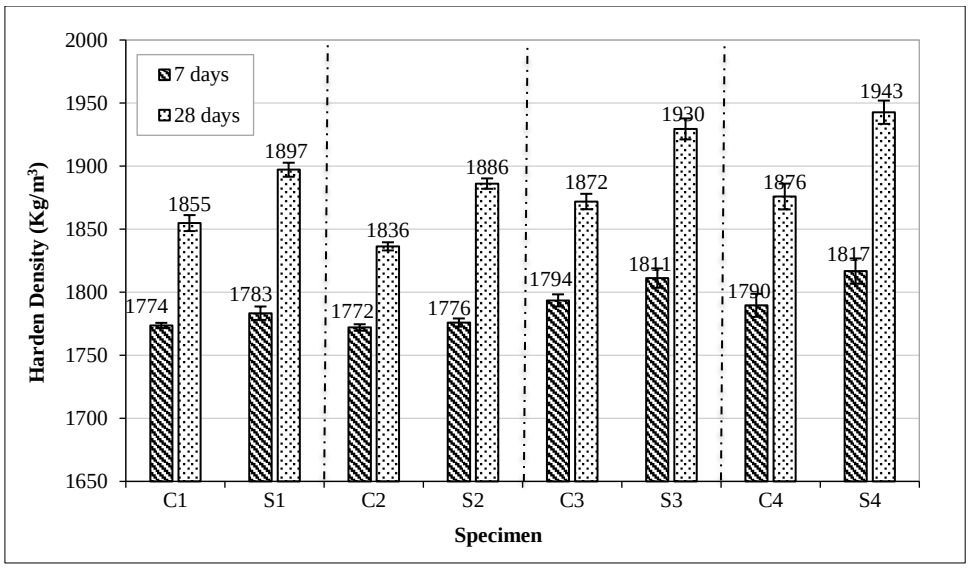

Figure 11. Graph of hardened density values at 7 and 28 days

Porosity is the volume of voids within cementitious composites and plays a critical role in influencing durability, permeability, and mechanical performance. Lower porosity typically leads to increased density, water resistance, and long-term durability [66]. In this study, porosity was determined by the water absorption method, conducted in conjunction with hardened density measurement in accordance with BS EN 1015-10 [50], where specimens were oven-dried to constant mass, then saturated in water. The open porosity was calculated from the mass difference between dry and saturated conditions (and, where applicable, immersed mass). Because this approach primarily captures connected (water-accessible) pores, the reported porosity trends should be interpreted as changes in open pore volume.

Figure 12 shows that the GFRCMs exhibit substantially reduced porosity compared to the control specimens, with S4 exhibiting the lowest porosity at 4.08%. At 28 days, the porosity ranking for GFRCMs is recorded as follows: S2 > S1 > S3 > S4. This observed phenomenon in GFRCMs was mainly due to enhanced interfacial bonding between the cement paste and aggregates, which was facilitated by glass fibres [67]. Nonetheless, the degree of porosity reduction was influenced by the mixing sequence, highlighting the importance of fibre dispersion in the formation of voids. The S4 specimen (lowest porosity) utilised a staggered water addition method that improved fibre dispersion and cement particle coating while reducing excess water pockets and entrapped air. These features contributed to lower void content, resulting in a denser microstructure characterised by fewer interconnected pores. Likewise, S1 and S2 exhibited greater porosity, presumably due to less regulated incorporation, leading to uneven fibre distribution and increased void formation. Overall, S3, employing a gradual water addition method, exhibited lower porosity than S1 and S2, confirming that controlled water incorporation improves compaction and minimises voids.

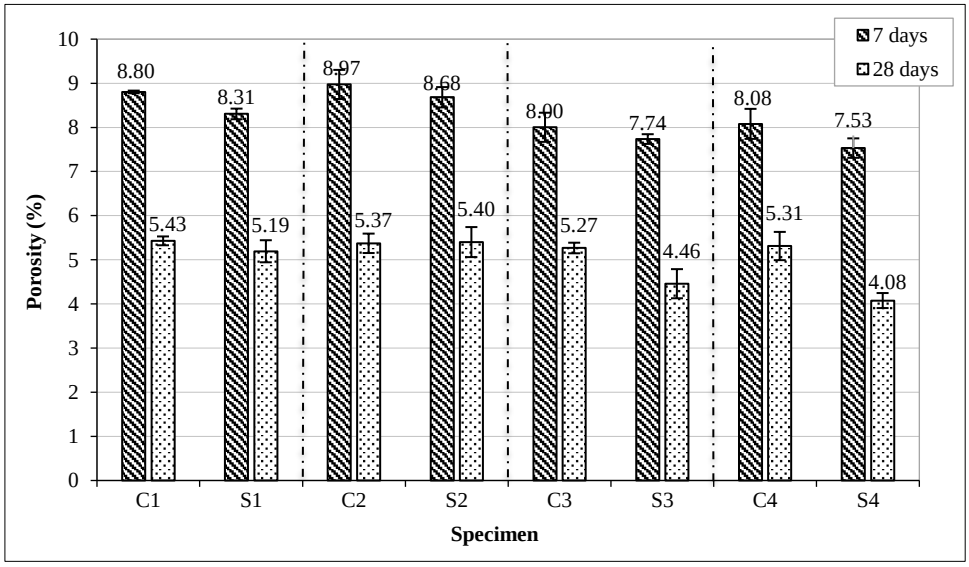

Figure 12. Graph of porosity values at 7 and 28 days

Figure 13 illustrates the correlation between hardened density and porosity, showing that higher specimen density corresponds to lower porosity. The trend line fitted to the data points indicated a considerable negative linear relationship between the variables, with a coefficient of determination (R^2) of 0.8035.

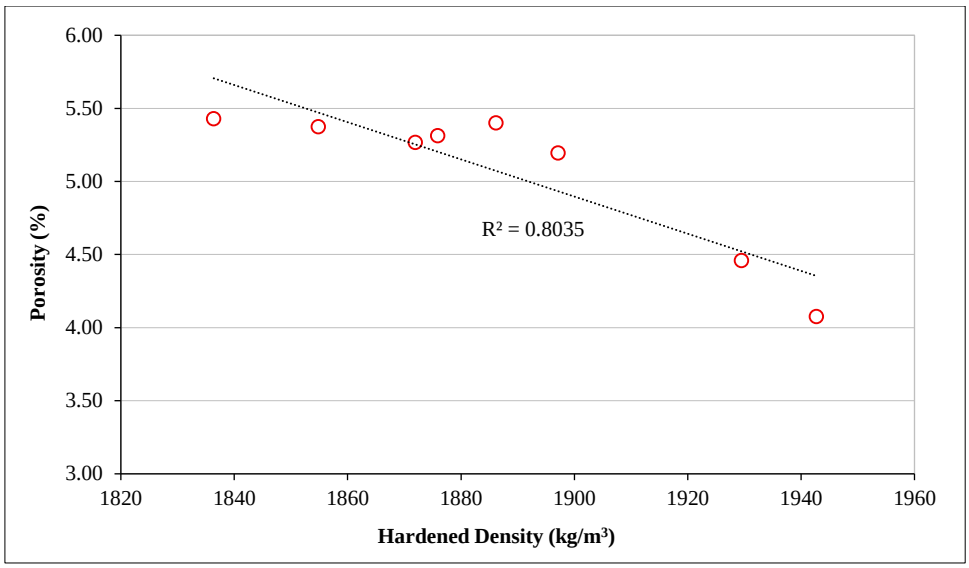

Figure 13. Graph of porosity versus hardened density

4.4. Compressive Strength

Compressive strength commonly indicates the load-bearing capacity of cementitious materials while serving as a critical measure of their performance [68]. This study then observed that the 7- and 28-day compressive strengths of GFRCMs exceeded those of the control specimens, demonstrating that the addition of glass fibres affected the mortar's mechanical characteristics. Previous studies also contended that glass fibres could improve interfacial bonding and micro-crack resistance, potentially aiding in strength development [8, 16].

Figure 14 presents the compressive strength data for the control specimens at 28, with values of 8.73 MPa for C1 and C2, 9.11 MPa for C3, and 9.13 MPa for C4. Meanwhile, the GFRCM data at 28 days for S1, S2, S3, and S4 were 11.83, 10.77, 11.95, and 15.88 MPa, respectively. This study then concluded that S4 and S2 presented the maximum and minimum compressive strengths, respectively. Notably, the reduced strength in S1 and S2 was due to inadequate fibre dispersion, leading to weak points and an uneven matrix structure [22-25]. In contrast, the enhanced strength of S3 is associated with improved dispersion resulting from incremental water addition. The superior performance of S4 is most consistently explained by the combined effects of reduced void content, improved fibre distribution, and enhanced fibre–matrix bonding due to more effective paste coating during staged water addition. Improved coating facilitates more efficient stress transfer and delays microcrack coalescence under compressive loading, while the staged process likely reduces fibre entanglement and promotes a more uniform, random distribution. Overall, the exceptional performance of S4 reflects the synergistic influence of void reduction, improved interfacial efficiency, and enhanced fibre dispersion [36]. These findings are consistent with previous research by Gyawali [36], which demonstrated that staged water incorporation improves fibre dispersion and compressive performance in fibre-reinforced mortars.

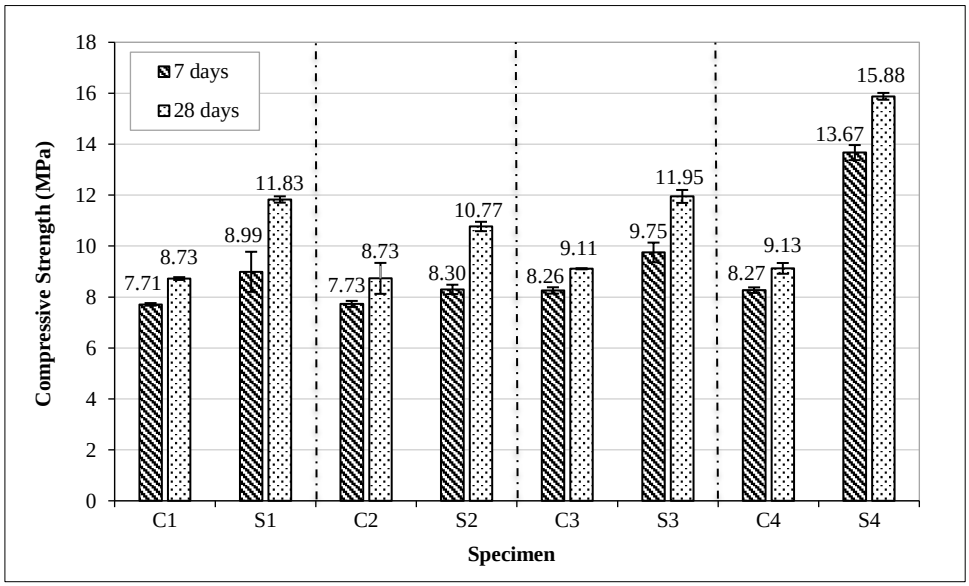

Figure 14. Graph of compressive strength values at 7 and 28 days

Figure 15 illustrates a linear correlation between compressive strength and hardened density. The data indicated that denser specimens exhibited higher compressive strengths, with a significant correlation (R^2 = 0.8184). Hence, this outcome implied that increased density could enhance load resistance, highlighting the importance of mixing sequences to optimise density and mechanical performance.

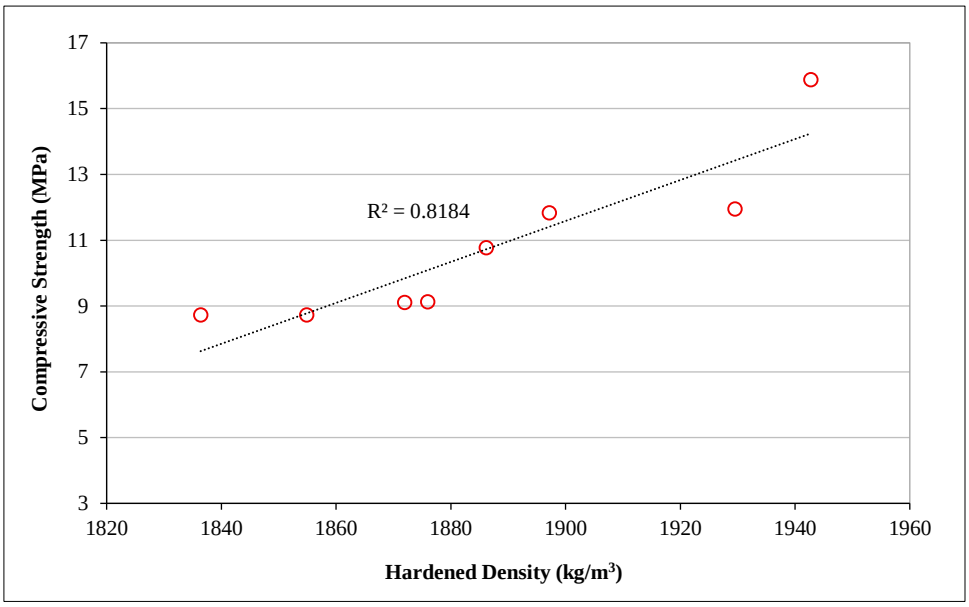

Figure 15. Graph of compressive strength versus hardened density

4.5. Flexural Strength

Flexural strength quantifies a material's ability to withstand deformation under an applied load [69]. This study then observed that the GFRCMs had greater flexural strength than the control specimens at 28 days. Figure 16 shows that the control and GFRCMs exhibit larger and minor cracks, respectively. This finding indicated that glass fibres contributed to the restriction of crack propagation, consistent with earlier studies on the crack-bridging effect of fibres in cementitious composites [8, 16].

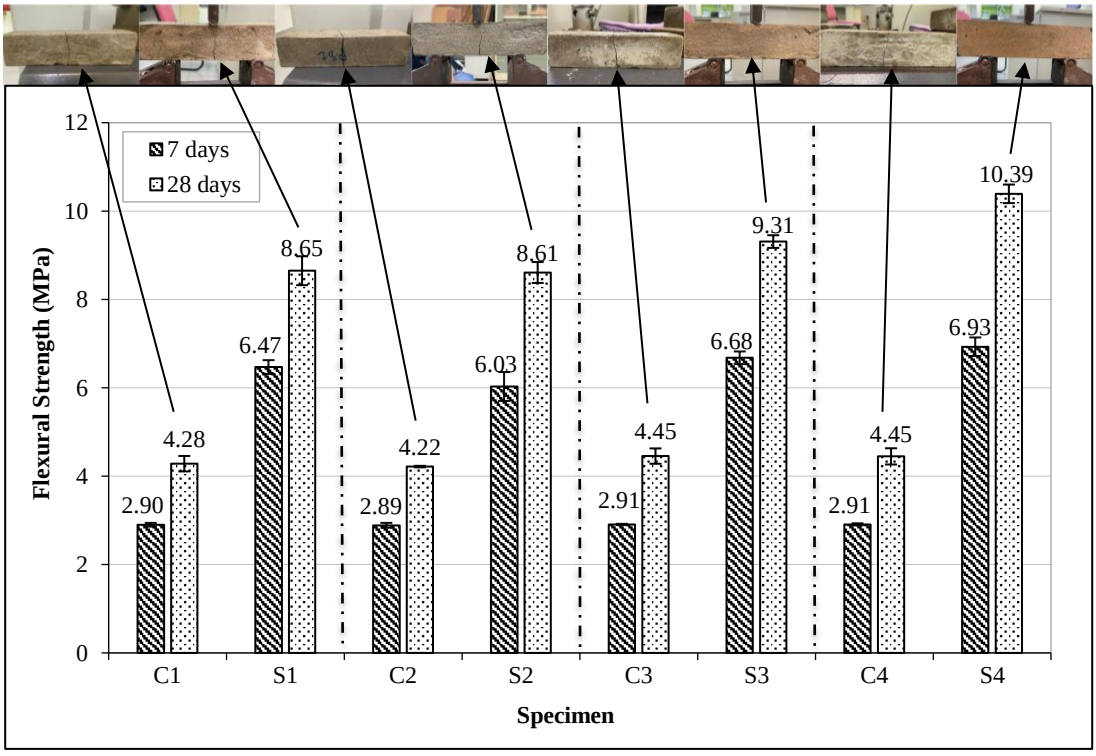

Figure 16. Graph of flexural strength values at 7 and 28 days

The flexural strength values for the control specimens at 28 days are as follows: C1 (2.95 MPa), C2 (4.22 MPa), C3 (4.45 MPa), and C4 (4.45 MPa). Comparatively, the flexural strength values for S1, S2, S3, and S4 were 8.65, 8.61, 9.31, and 10.39 MPa, respectively. This study found that the S4 specimen demonstrated the greatest flexural strength, whereas the S2 specimen showed the least. The S1, S3, and S4 specimens were positioned between the S2 and S4 specimens. Thus, the reduced flexural strength in S1 and S2 indicated that inadequate fibre dispersion led to weak zones within the matrix, diminishing its capacity to withstand tensile stress. Conversely, S3 and S4 exhibited superior performance, which was presumably attributable to enhanced fibre-matrix bonding. This process could then improve the load transfer and fracture resistance [23, 25]. Overall, the mixing sequence employed in S4 likely enhanced fibre distribution, mitigated stress concentrations, and improved overall toughness [36].

These findings are consistent with the work of Gyawali [36], who reported that a gradual water addition method enhanced fibre distribution and paste coating, resulting in higher flexural performance compared with conventional single-step mixing [36]. The present results follow a similar trend, where the staged-water sequence (S4) yielded the highest 28-day flexural strength. This outcome further supports the premise that improved fibre dispersion and reduced fibre clustering enhance crack-bridging efficiency and load transfer under bending.

5. Correlation between Fibre Dispersion and Engineering Properties

5.1. SEM

Figure 17 depicts the distribution of glass fibres within the cementitious mortar matrix across various mixing sequences. Notable clumping of fibres was then observed in S1 and S2, suggesting significant aggregation issues that could lead to weak spots and undermine the mechanical integrity of the mortar [see Figures 17-a and 17-b]. Alternatively, improved fibre dispersion was observed for S3 and S4, as evidenced by a more uniform distribution of fibres (no significant clumping). [see Figures 17-c and 17-d]. This study then verified that a more uniform dispersion occurred in S3 and S4 compared to S1 and S2. Consequently, a positive correlation was demonstrated between fibre dispersion uniformity and the strength of the GFRCMs.

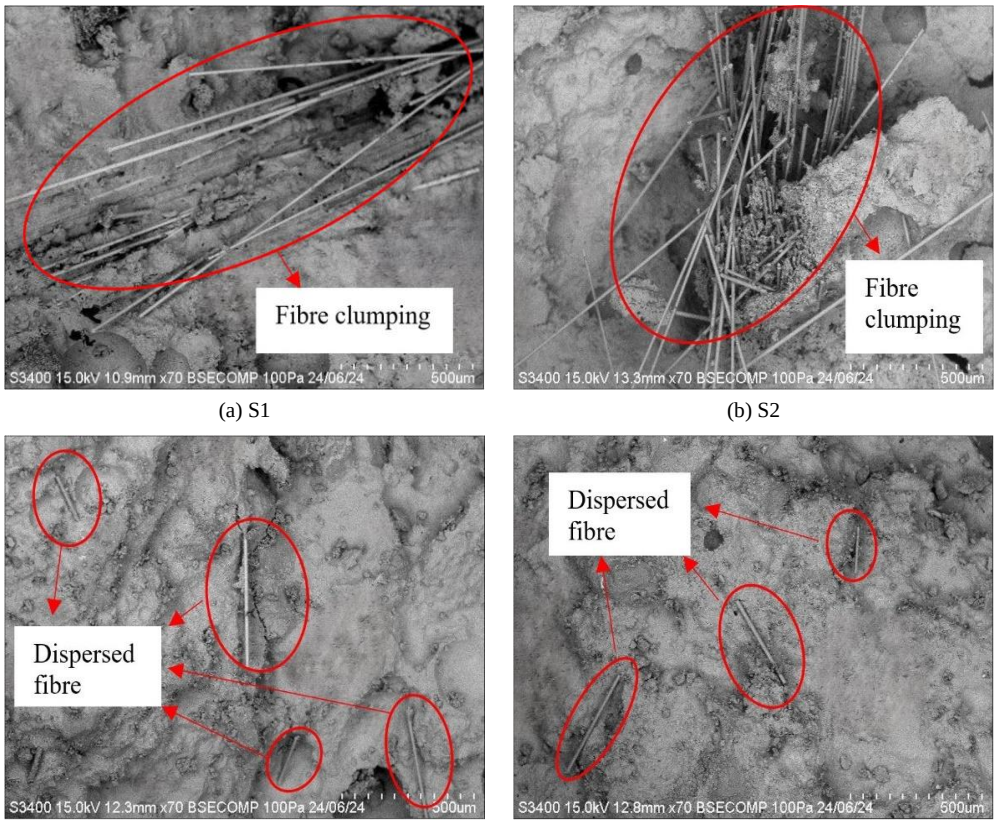

(a) S1 (b) S2

(c) S3 (d) S4

Figure 17. The SEM images of various GFRCMs involving (a) S1, (b) S2, (c) S3, and (d) S4

5.2. FDA

Figure 18 illustrates the dispersion coefficients for various GFRCMs (ascending order): S4 (0.685), S3 (0.680), S1 (0.588), and S2 (0.476). Improved engineering properties were then determined for S4 based on its most uniform fibre distribution. Nonetheless, S2 demonstrated inferior mechanical characteristics due to its least uniform distribution. This

study also verified that the sequence of fibre dispersion (S4 > S3 > S1 > S2) corresponded with the hierarchy of engineering properties, as evidenced by SEM findings. Therefore, a substantial relationship between fibre dispersion and mechanical properties was concluded in this study.

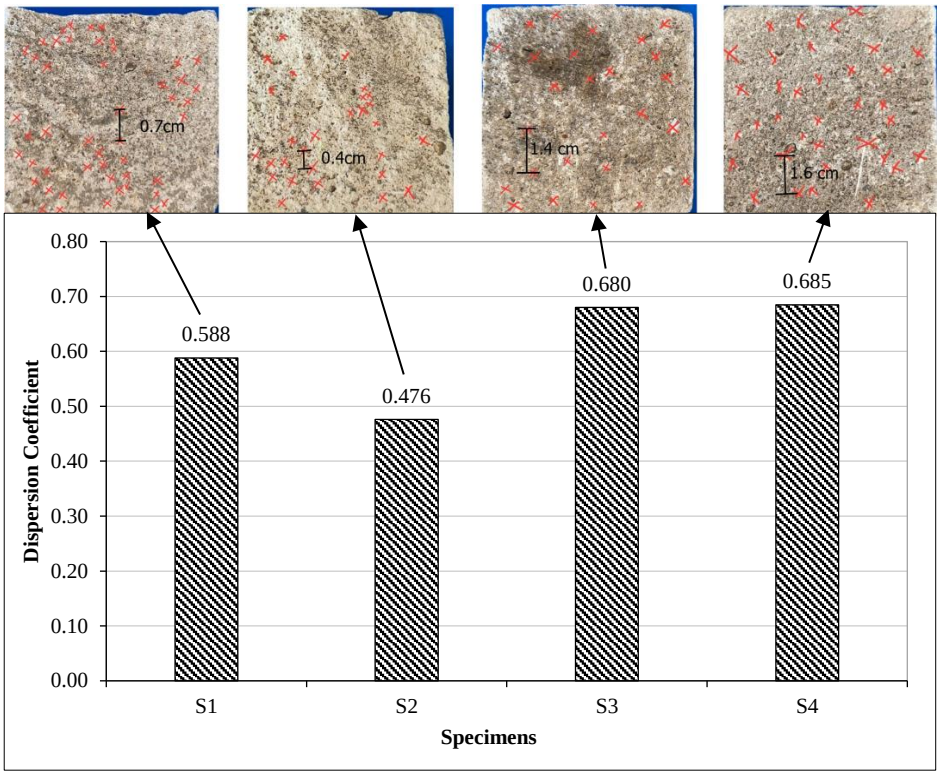

Figure 18. Fibre Dispersion Coefficient of GFRCM Specimens

6. Conclusion

This study examined the effect of four mixing sequences on the engineering properties and fibre dispersion of glass fibre-reinforced cementitious mortar (GFRCMs). In general, fibre incorporation reduced the spread flow due to increased internal friction and higher water demand. This reduction was most pronounced in S1 and S2, where fibres were introduced into either dry or fully wetted mixes without staged wetting, promoting early fibre interaction and increased mixture viscosity. Fibre addition also shortened the setting time, which is attributed to reduced free water availability and interfacial interactions at the hydrophilic fibre surface. In the hardened state, the mixing sequence exerted a decisive influence, with S4 (two-stage water addition) producing the densest matrix and the lowest open porosity, indicating improved compaction and fewer interconnected voids.

Mechanical testing further confirmed that enhanced fibre dispersion translated into superior performance. At 28 days, S4 achieved the highest compressive strength (15.88 MPa) and flexural strength (10.39 N/mm²), whereas S2 exhibited the lowest strengths, consistent with its poorer dispersion quality. SEM observations and fibre distance analysis corroborated this trend, with dispersion coefficients ranking S4 > S3 > S1 > S2, and S4 attaining the highest β value (0.685). Strong correlations between hardened density and porosity (R^2 = 0.8035) and between density and compressive strength (R^2 = 0.8184) indicate that strength enhancement is primarily governed by the reduction of voids achieved through uniform fibre distribution and effective paste coating.

Overall, the findings demonstrate that introducing two-stage water addition is an effective mixing sequence to minimise fibre clumping, stabilise flowability, enhance mechanical properties, and maximise the reinforcing benefits of glass fibres in cementitious mortars.

7. Declarations

7.1. Author Contributions

Conceptualization, A.M.S. and A.N.R.; methodology, AM.S. and A.N.R.; validation, A.M.S., A.N.R., A.H.B., S.M.I.S.Z., G.L., Z.D., and R.S.; formal analysis, A.M.S., S.M.I.S.Z., and A.N.R.; investigation, A.M.S., A.H.B., and A.N.R.; resources, A.M.S, S.M.I.S.Z, and A.N.R.; data curation, A.M.S.; writing—original draft preparation, A.M.S.; writing—review and editing, A.M.S. and A.N.R.; visualization, A.M.S.; supervision, A.N.R., S.M.I.S.Z., and R.S.; project administration, A.N.R.; funding acquisition, A.N.R. and R.S. All authors have read and agreed to the published version of the manuscript.

7.2. Data Availability Statement

The data presented in this study are available in the article.

7.3. Funding

This research was financially supported by the Malaysian Ministry of Higher Education (Grant No. FRGS/1/2024/TK06/UMS/02/1).

7.4. Conflicts of Interest

The authors declare no conflict of interest.

8. References

[1] Li, V. C. (2003). On Engineered Cementitious Composites (ECC). Journal of Advanced Concrete Technology, 1(3), 215–230. doi:10.3151/jact.1.215.

[2] Zhou, Y., Guo, W., Zheng, S., Xing, F., Guo, M., & Zhu, Z. (2023). Development of Sustainable Engineered Cementitious Composites by Incorporating Local Recycled Fine Aggregate. Polymers, 15(12), 2701. doi:10.3390/polym15122701.

[3] Xu, L. Y., Huang, B. T., Lao, J. C., Yao, J., Li, V. C., & Dai, J. G. (2023). Tensile over-saturated cracking of Ultra-High-Strength Engineered Cementitious Composites (UHS-ECC) with artificial geopolymer aggregates. Cement and Concrete Composites, 136, 104896. doi:10.1016/j.cemconcomp.2022.104896.

[4] Arslan, K. M., & Karagüler, M. E. (2024). Shrinkage cracking and mechanical properties of cementitious composites produced with multiwall carbon nano tubes and different types of polypropylene fibres. Construction and Building Materials, 420, 135599. doi:10.1016/j.conbuildmat.2024.135599.

[5] Sapawi, A. M., Rizalman, A. N., Taha, N. A., Taharin, M. R., & Matlan, S. J. (2025). Effects of fiber content, mixing sequence, and mixing time on the properties of fiber-reinforced cementitious composites: A review. Cutting-Edge Advances in Nanofibers and Fibers: Shaping Future Applications: IGI Global Scientific Publishing, 435–471. doi:10.4018/979-8-3373-0230-0.ch013.

[6] Kim, D. joo, Naaman, A. E., & El-Tawil, S. (2008). Comparative flexural behavior of four fiber reinforced cementitious composites. Cement and Concrete Composites, 30(10), 917–928. doi:10.1016/j.cemconcomp.2008.08.002.

[7] Chandrathilaka, E. R. K., Baduge, S. K., Mendis, P., & Thilakarathna, P. S. M. (2021). Structural applications of synthetic fibre reinforced cementitious composites: A review on material properties, fire behaviour, durability and structural performance. Structures, 34, 550–574. doi:10.1016/j.istruc.2021.07.090.

[8] Zhang, M., & Matinlinna, J. P. (2012). E-Glass Fiber Reinforced Composites in Dental Applications. Silicon, 4(1), 73–78. doi:10.1007/s12633-011-9075-x.

[9] Tatar, J., & Milev, S. (2021). Durability of externally bonded fiber-reinforced polymer composites in concrete structures: A critical review. Polymers, 13(5), 1–26. doi:10.3390/polym13050765.

[10] AGY. (2021). High strength glass fibers. AGY – Glass Fibre Innovations, United States. Available online: https://www.agy.com/wp-content/uploads/2022/03/AGY_HighStBro_HR.pdf (accessed on March 2026).

[11] Chawla, K. K. (2016). Glass Fibers. Encyclopedia of Materials: Technical Ceramics and Glasses, 676–680. doi:10.1016/b978-0-12-818542-1.02325-0.

[12] Zainal, S. M. I., Wong, C. W., Rizalman, A. N., Majain, N., Lim, C. H., & Sarbatly, R. (2024). Characterization and mixing sequence to enhance glass fiber performance in cement mixture. Materials and Structures/Materiaux et Constructions, 57(7), 163. doi:10.1617/s11527-024-02429-4.

[13] Kasagani, H., & Rao, C. B. K. (2018). Effect of graded fibers on stress strain behaviour of Glass Fiber Reinforced Concrete in tension. Construction and Building Materials, 183, 592–604. doi:10.1016/j.conbuildmat.2018.06.193.

[14] Alsadey, S., Abdallateef, M., Mohamed, M., & Milad, A. (2021). Investigating Behaviour of Reinforced Concrete with Glass Fibre. Jurnal Kejuruteraan, 33(3), 551–557. doi:10.17576/jkukm-2021-33(3)-16.

[15] Zhou, B., Zhang, M., Wang, L., & Ma, G. (2021). Experimental study on mechanical property and microstructure of cement mortar reinforced with elaborately recycled GFRP fiber. Cement and Concrete Composites, 117, 103908. doi:10.1016/j.cemconcomp.2020.103908.

[16] Boukni, B., Khouadjia, M. L. K., & Bensalem, S. (2024). Effect of glass fibers on performance of mortar and concrete. Studies in Engineering and Exact Sciences, 5(1), 2509–2528. doi:10.54021/seesv5n1-124.

[17] Sapawi, A. M., Rizalman, A. N., Asrah, H., Lim, C. H., & Amaludin, A. E. (2025). An overview of the effects of incorporating glass fiber on mechanical properties of cementitious composites. Cutting-Edge Advances in Nanofibers and Fibers: Shaping Future Applications: IGI Global, 473–501. doi:10.4018/979-8-3373-0230-0.ch014.

[18] Choi, Y., & Yuan, R. L. (2005). Experimental relationship between splitting tensile strength and compressive strength of GFRC and PFRC. Cement and Concrete Research, 35(8), 1587–1591. doi:10.1016/j.cemconres.2004.09.010.

[19] Kumar, D., Rex, L. K., Sethuraman, V. S., Gokulnath, V., & Saravanan, B. (2020). High performance glass fiber reinforced concrete. Materials Today: Proceedings, 33, 784–788. doi:10.1016/j.matpr.2020.06.174.

[20] Tibebu, A., Mekonnen, E., Kumar, L., Chimdi, J., Hailu, H., & Fikadu, N. (2022). Compression and workability behavior of chopped glass fiber reinforced concrete. Materials Today: Proceedings, 62, 5087–5094. doi:10.1016/j.matpr.2022.02.427.

[21] Wu, C., He, X., Zhao, X., He, L., Song, Y., & Zhang, X. (2022). Effect of Fiber Content on Mechanical Properties and Microstructural Characteristics of Alkali Resistant Glass Fiber Reinforced Concrete. Advances in Materials Science and Engineering, 2022, 1–19. doi:10.1155/2022/1531570.

[22] Ferrara, L., Park, Y.-D., & Shah, S. P. (2008). Correlation among Fresh State Behavior, Fiber Dispersion, and Toughness Properties of SFRCs. Journal of Materials in Civil Engineering, 20(7), 493–501. doi:10.1061/(asce)0899-1561(2008)20:7(493).

[23] Sharafeddin, F., Alavi, A., & Talei, Z. (2013). Flexural strength of glass and polyethylene fiber combined with three different composites. Journal of Dentistry (Shiraz, Iran), 14(1), 13–19.

[24] Mahdi, R. S. (2014). Experimental study effect of using glass fiber on cement mortar. Journal of Babylon University/Engineering Sciences, 22(1), 162–181.

[25] Hilles, M. M., & Ziara, M. M. (2019). Mechanical behavior of high strength concrete reinforced with glass fiber. Engineering Science and Technology, an International Journal, 22(3), 920–928. doi:10.1016/j.jestch.2019.01.003.

[26] Liu, S., & Fall, M. (2024). The significance of mixing time in the development of the engineering properties of cemented fiber-reinforced tailings materials. Journal of Building Engineering, 96, 110648. doi:10.1016/j.jobe.2024.110648.

[27] Felekoglu, B., Tosun-Felekoglu, K., Ranade, R., Zhang, Q., & Li, V. C. (2014). Influence of matrix flowability, fiber mixing procedure, and curing conditions on the mechanical performance of HTPP-ECC. Composites Part B: Engineering, 60, 359–370. doi:10.1016/j.compositesb.2013.12.076.

[28] Czoboly, O., & Balazs, G. L. (n.d.). Influence of Mixing Time to the Properties of Steel Fibres and Steel Fibres Reinforced Concrete. Concrete Structures: Journal of the Hungarian Group of Fib, 17, 23–28.

[29] Cazacliu, B., Loukili, A., Abdi, B., & Le Roy, R. (2006). Mixing of an ultra-high-performance fiber-reinforced concrete. Bulletin Des Laboratoires des Ponts et Chaussees, 261–262, 261–262.

[30] Lerch, J. O., Bester, H. L., Van Rooyen, A. S., Combrinck, R., de Villiers, W. I., & Boshoff, W. P. (2018). The effect of mixing on the performance of macro synthetic fibre reinforced concrete. Cement and Concrete Research, 103, 130–139. doi:10.1016/j.cemconres.2017.10.010.

[31] Zeyad, A. M., & Almalki, A. (2020). Influence of mixing time and superplasticizer dosage on self-consolidating concrete properties. Journal of Materials Research and Technology, 9(3), 6101–6115. doi:10.1016/j.jmrt.2020.04.013.

[32] Pothisiri, T., & Soklin, C. (2014). Effects of mixing sequence of polypropylene fibers on spalling resistance of normal strength concrete. Engineering Journal, 18(3), 55–63. doi:10.4186/ej.2014.18.3.55.

[33] Zhou, J., Qian, S., Ye, G., Copuroglu, O., Van Breugel, K., & Li, V. C. (2012). Improved fiber distribution and mechanical properties of engineered cementitious composites by adjusting the mixing sequence. Cement and Concrete Composites, 34(3), 342–348. doi:10.1016/j.cemconcomp.2011.11.019.

[34] França, M. S. de, Cardoso, F. A., & Pileggi, R. G. (2016). Influence of the addition sequence of PVA-fibers and water on mixing and rheological behavior of mortars. Revista IBRACON de Estruturas e Materiais, 9(2), 226–243. doi:10.1590/s1983-41952016000200005.

[35] Gao, J., Wang, Z., Zhang, T., & Zhou, L. (2017). Dispersion of carbon fibers in cement-based composites with different mixing methods. Construction and Building Materials, 134, 220–227. doi:10.1016/j.conbuildmat.2016.12.047.

[36] Gyawali, T. R. (2018). Investigation on mixing process for the development of high ductile mortar containing thin and short fibers. International Journal of Science and Research, 9(1), 8–15.

[37] Anthony, E. N., Rizalman, A. N., Thurairajah, A. R., Zainal, S. M. I. S., & Sulaiman, M. F. (2024). Mixing Sequence Effect of Cement Composites with Carbon Fibres. IIUM Engineering Journal, 25(1), 142–152. doi:10.31436/iiumej.v25i1.2983.

[38] Thurairajah, A. R., Rizalman, A. N., Anthony, E. N., Dagul, M. D., & Sarbatly, R. (2024). Engineering Properties of Cement-Paste with Polypropylene and Carbon Fibres. Journal of Advanced Research in Applied Mechanics, 115(1), 98–106. doi:10.37934/aram.115.1.98106.

[39] Boulekbache, B., Hamrat, M., Chemrouk, M., & Amziane, S. (2010). Flowability of fibre-reinforced concrete and its effect on the mechanical properties of the material. Construction and Building Materials, 24(9), 1664–1671. doi:10.1016/j.conbuildmat.2010.02.025.

[40] Saidani, M., Saraireh, D., & Gerges, M. (2016). Behaviour of different types of fibre reinforced concrete without admixture. Engineering Structures, 113, 328–334. doi:10.1016/j.engstruct.2016.01.041.

[41] Chen, Y., Matalkah, F., Weerasiri, R. R., Balachandra, A. M., & Soroushian, P. (2017). Dispersion of Fibers in Ultra-High-Performance Concrete. ACI Concrete International, 39(12), 45–50. doi:10.14359/51701341.

[42] Mohamed, O., & Zuaiter, H. (2024). Fresh Properties, Strength, and Durability of Fiber-Reinforced Geopolymer and Conventional Concrete: A Review. Polymers, 16(1), 141. doi:10.3390/polym16010141.

[43] ASTM C150/C150M-22. (2007). Standard specification for Portland cement. ASTM International, Pennsylvania, United States.

[44] ASTM C494/C494M-05a. (2006). Standard specification for chemical admixtures for concrete. ASTM International, Pennsylvania, United States.

[45] BS EN 934-2:2009+A1:2012. (2012). Admixtures for concrete, mortar and grout – Concrete admixtures: Definitions, requirements, conformity, marking and labelling. European Committee for Standardization, Brussels, Belgium.

[46] ASTM C1602/C1602M-06. (2006). Standard specification for mixing water used in the production of hydraulic cement concrete. ASTM International, Pennsylvania, United States.

[47] ASTM C109/C109M-02. (1999). Standard test method for compressive strength of hydraulic cement mortars (using 2-in. or [50 mm] cube specimens). ASTM International, Pennsylvania, United States.

[48] ASTM C1437-20. (2020). Standard test method for flow of hydraulic cement mortar. ASTM International, Pennsylvania, United States.

[49] ASTM C191-08. (2009). Standard test method for time of setting of hydraulic cement by Vicat needle. ASTM International, Pennsylvania, United States.

[50] BS EN 1015-10. (1999). Methods of test for mortar for masonry – Determination of dry bulk density of hardened mortar. British Standards Institution, London, United Kingdom.

[51] ASTM C348-02. (2002). Standard test method for flexural strength of hydraulic-cement mortars. ASTM International, Pennsylvania, United States.

[52] ASTM C128-07a. (2007). Standard test method for density, relative density (specific gravity), and absorption of fine aggregate. ASTM International, Pennsylvania, United States.

[53] Betterman, L. R., Ouyang, C., & Shah, S. P. (1995). Fiber-matrix interaction in microfiber-reinforced mortar. Advanced Cement Based Materials, 2(2), 53–61. doi:10.1016/1065-7355(95)90025-X.

[54] Yin, S., Tuladhar, R., Shi, F., Combe, M., Collister, T., & Sivakugan, N. (2015). Use of macro plastic fibres in concrete: A review. Construction and Building Materials, 93, 180–188. doi:10.1016/j.conbuildmat.2015.05.105.

[55] Lawler, J. S., Wilhelm, T., Zampini, D., & Shah, S. P. (2003). Fracture processes of hybrid fiber-reinforced mortar. Materials and Structures, 36(3), 197–208. doi:10.1007/bf02479558.

[56] Li, Z., Liu, J., Yuan, Y., Li, E., & Wang, F. (2017). Effects of surface fluoride-functionalizing of glass fiber on the properties of PTFE/glass fiber microwave composites. RSC Advances, 7(37), 22810–22817. doi:10.1039/c7ra02715j.

[57] ASTM D2487-06. (2008). Standard practice for classification of soils for engineering purposes (unified soil classification system). ASTM International, Pennsylvania, United States.

[58] Yang, Z., Yuan, K., Meng, J., Zhang, X., Tang, D., & Hu, M. (2021). Why thermal conductivity of CaO is lower than that of CaS: a study from the perspective of phonon splitting of optical mode. Nanotechnology, 32(2), 25709. doi:10.1088/1361-6528/abbb4c.

[59] Lipatov, Y. V., Gutnikov, S. I., Manylov, M. S., & Lazoryak, B. I. (2012). Effect of ZrO 2 on the alkali resistance and mechanical properties of basalt fibers. Inorganic Materials, 48(7), 751–756. doi:10.1134/S0020168512060106.

[60] Zhang, H. (2011). Cement. Building Materials in Civil Engineering, 46–423. doi:10.1533/9781845699567.46.

[61] Horkoss, S., Lteif, R., & Rizk, T. (2011). Influence of the clinker SO3 on the cement characteristics. Cement and Concrete Research, 41(8), 913–919. doi:10.1016/j.cemconres.2011.04.015.

[62] Okoh, J. S., & Dim, P. E. (2024). P066 - Investigation on the Effect of Iron Oxide (Feo_3) Pigment on the Production of Coloured Cement for. International Journal of Novel Research and Development, 9(7), 66.

[63] Ahmad, J., González-Lezcano, R. A., Majdi, A., Ben Kahla, N., Deifalla, A. F., & El-Shorbagy, M. A. (2022). Glass Fibers Reinforced Concrete: Overview on Mechanical, Durability and Microstructure Analysis. Materials, 15(15), 5111. doi:10.3390/ma15155111.

[64] Erdem, T. K., Turanli, L., & Erdogan, T. Y. (2003). Setting time: An important criterion to determine the length of the delay period before steam curing of concrete. Cement and Concrete Research, 33(5), 741–745. doi:10.1016/S0008-8846(02)01058-X.

[65] Rezania, M., Moradnezhad, H., Panahandeh, M., Rahimpoor Kami, M. J., Rahmani, A., & Hosseini, B. V. (2020). Effects of Diethanolamine (DEA) and Glass Fibre Reinforced polymer (GFRP) on setting time and mechanical properties of shotcrete. Journal of Building Engineering, 31, 101343. doi:10.1016/j.jobe.2020.101343.

[66] Abdullah, E. C., & Geldart, D. (1999). The use of bulk density measurements as flowability indicators. Powder Technology, 102(2), 151–165. doi:10.1016/S0032-5910(98)00208-3.

[67] Lin, C., Kanstad, T., Jacobsen, S., & Ji, G. (2023). Bonding property between fiber and cementitious matrix: A critical review. Construction and Building Materials, 378, 131169. doi:10.1016/j.conbuildmat.2023.131169.

[68] Telrandhe, S. (2024). Everything you need to learn about the compressive strength of concrete. Sakshi Chem Sciences, India. Available online: https://www.sakshichemsciences.com/compressive-strength-of-concrete/ (accessed on March 2026).

[69] Pal, T., Pramanik, S., Verma, K. D., Naqvi, S. Z., Manna, P. K., & Kar, K. K. (2021). Fly ash-reinforced polypropylene composites. Handbook of Fly Ash, 243–270. doi:10.1016/B978-0-12-817686-3.00021-9.